International Journal of ChemTech Research
CODEN (USA): IJCRGG ISSN: 0974-4290
Vol.9, No.03 pp 412-423, 2016

Adsorption of crystal violet dye by *Fugas Sawdust* from aqueous solution

Aseel M. Aljeboree

Department of Chemistry, College of Sciences for Girls, Babylon University, Hilla, Iraq

Abstract: The adsorption of textile dyes (Basic crystal violet dye as a model (CV)) from aqueous solution by Fugas Sawdust Carton (*FSC*) was studied. The adsorbent before and after adsorption was characterized by FTIR, and SEM, respectively. The effect of different experimental parameters such as initial concentration of CV dye (5-100 mg L^{-1}), particle size (50-100 μm), initial pH 2-10 of aqueous solution, adsorbent dose (0.005 -0.1 g) and solution temperature (283K - 313K) on the adsorption of CV were investigated.
Third adsorption isotherms were used to model the equilibrium adsorption of crystal violet dye on *FSC* adsorbent (Langmuir, Freundlich, and Temkin). By considering the experimental results and adsorption models applied in this study, it can be concluded that equilibrium data were represented well by all isotherm equations under study. The applicability of the isotherm's model for the present data follows the order: Freundlich> Temkin> Langmuir. Based on the calculated thermodynamic parameters such as enthalpy (ΔH°), entropy (ΔS°), and Gibbs free energy changes (ΔG°), it is noticeable that the sorption of CV dye onto *FSC* was a spontaneous and endothermic process.
Key words: Fugas Sawdust *FSC*, crystal violet dye, Adsorption isotherm, thermodynamic parameters.

Introduction

Textile wastewaters have a large amount of suspended solids (SS), in addition to COD (chemical oxygen demand), BOD (biochemical oxygen demand), heat, color, acidity, basicity and other inorganic contaminants. Most pollutants, except color, can be removed by conventional sewage treatment works[1]. Dyes are difficult to eliminate due to their synthetic origin and complex structure which makes them very stable[2]. The presence of even very low concentrations of dyes in effluents is highly visible and undesirable[3]. Moreover, their presence reduces aquatic diversity by blocking the passage of light through the water, there by precluding the photosynthesis of aquatic flora[4]. There is a large variety of dyes (acid, basic, reactive, direct, dispersive, sculpture and metallic dyes) that fall into the cationic, non-ionic or anionic category. Direct, acid and reactive dyes are anionic whereas basic dyes are cationic. The highest levels of toxicity have been found in basic and diazo direct dyes[5].

The dye wastewater has long been a major environmental problem all over the world. The main sources of dye wastewater are from textile, dying, printing and other related industries[6]. Among various dyes, Crystal Violet, also known as C.I. Basic Violet 3, is a kind of cationic triphenylmethane dye. It is widely used for textile dying, paper printing, biological staining, dermatological agent, veterinary medicine, intestinal parasites and fungus, etc.[7] Crystal Violet is a mutagen and mitotic poison, and its presence in water will cause a serious risk to aquatic life and constitute a potential human health hazard. Current treatment methods for dye

wastewater include physical, chemical, and biological methods, and so on. Various removal methods have been studied by photocatalytic degradation[8-19],adsorption[20-27], chemical coagulation,[28] liquid membrane separation[29], electrolysis[30], and biological treatments[31]. However, these processes vary in their effectiveness, costs, and environmental impacts[32]. Among these processes, the adsorption process is much more competitive than other methods for its ready availability, lower cost, and wider range of applications.[33] In adsorption processes a porous solid (adsorbent) is used to capture soluble substances present in aqueous solution (dyes for instance).

Several adsorbents have shown good promise for dye removal from wastewater. Activated carbon is an effective but expensive adsorbent due to its high costs of manufacturing. This has led many workers to search for the use of cheap and efficient alternative materials. These include rice husk[34], apricot stones[35], hen feather waste, and coconut bunch waste[36], etc.

Therefore, the objective of this investigation was to explore the potential of *Fugas* Sawdust cartoon (*FSC*) as a low cost adsorbent for the removal of CV dye from aqueous solutions. The present study describes the effects of concentration of dye, initial solution pH, particle size, adsorbent dose, and temperature on CV adsorption rate have been investigated, isotherms, and thermodynamics were also evaluated and reported.

Experimental

Materials and methods

Crystal violet (CV) was obtained from Merck/ Germany. The respective chemical structures are shown in Fig. 1. The physicochemical properties of the dye are presented in Table 1. For experimentation all the solutions were prepared after dilution of the stock solution, which was prepared in distilled water. A stock solution of 500 mg/L was prepared by dissolving 0.5 g as an appropriate quantity of crystal violet dye (CV) in 1 L double distilled water. Working solutions of desired concentrations were prepared by successive dilution. The natural pH of CV dye solution was found to be 6.20

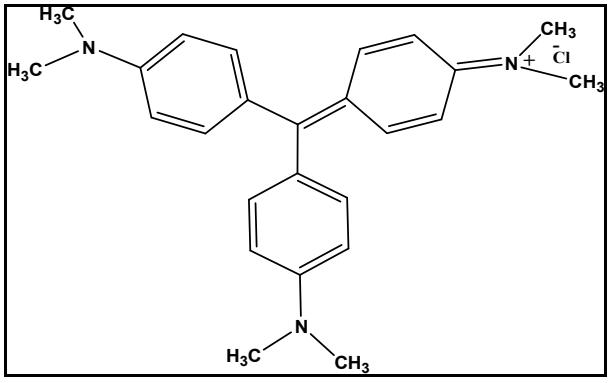

Fig. 1: Chemical structure of crystal violet dye

Table 1: Physico-chemical characteristics of the crystal violet dye.

Values	Parameters
407.98	Molecular weight
$C_{25}H_{30}N_3Cl$	Molecular formula
Basic Violet 3, Gentian Violet	Synonyms
N-[4-[Bis[4-dimethylamino)-phenyl]-methylene]-2,5-cyclo hexadien-1-ylidine]-N-methyl-methanaminium chloride	IUPAC name
589–594 nm	λ max

Preparation of activated *Fugas Sawdust cartoon* (*FSC*):

Fugas Sawdust cartoon (*FSC)* (also known a beech wood) in Iraq, was obtained from the carton factory Hilla/Iraq. The raw carton was sieved through a 3-2 mm sieve, washed repeatedly with distilled water to remove surface and soluble impurities, and dried at 100°C for 48 h. The dried carton (*FSC)* was not subjected to further processing or chemical treatment, which might enhance its adsorptive capacity in an attempt to evaluate the CV adsorption properties of a low-cost unprocessed sawdust, abundantly available in Hilla/Iraq. The clean biomass are mechanically ground and sifted to get a powder with particle size <100, 75, and 50 μm.

Adsorption studies

Batch experiments were carried out to evaluate the effect of initial dye concentration, solution pH, particle size and temperature, for the removal of CV dye on (*FSC*) adsorbent from aqueous solutions. In all experiments except for the initial concentration, 50 mg *FSC* was added to 100 mL water solution of CV. with a choosen concentration of of CV dye. After stirring on a shaker for predetermined time intervals, the solution containing *FSC* and CV was treated with centrifugation for solid–liquid separation and then was diluted. The residual concentration of dye solution was determined using a calibration curve prepared at the corresponding maximum wavelength (593 nm) using a UV– visible spectrometer (UV mini 1240 shimadzu).

The effect of pH on dye removal was studied over a pH range of 2–10. The initial pH of the dye solution was adjusted by the addition of 0.05 N solution of HCl or NaOH. The concentration of CV dye solution ranged from 5 to 100 mg/L to investigate the adsorption isotherms. The sorption studies were also carried out at different temperatures (10, 25, and 40 °C) to determine the effect of temperature in order to evaluate the thermodynamic parameters.

The amount of adsorbed dye, qe (mg/g) was calculated by

$$q_e = \left(\frac{C_0 - C_e}{W}\right) * V \qquad (1)$$

where C_0 and C_e are the initial and equilibrium concentrations (mg/ L), respectively, V is the volume of dye solution (L), and W is the weight (g) of FSC adsorbent. The dye removal efficiencies under different conditions were calculated from the difference between the initial (without adsorbent) and equilibrium concentrations of the solution which was defined as:

$$E\% = \left(\frac{C_0 - C_e}{C_0}\right) * 100 \qquad (2)$$

3. Results and discussion

3.1. FT-IR characterization

The FSC adsorbent was characterized by FT-IR spectroscopy. FTIR spectra were collected in the mid - IR range from 4000 to 400 cm^{-1} with a resolution of 1 cm^{-1}. The FT-IR spectra of FSC before and after adsorption of CV are shown in Figure 2. The FT-IR pattern shows reduced in an intensity of bands after adsorption, also there is a real difference between FSC before and after interaction with CV which has been suggested a physical adsorption phenomenon occurs as a result of attractive forces between the FSC surface and CV under investigation.[37]

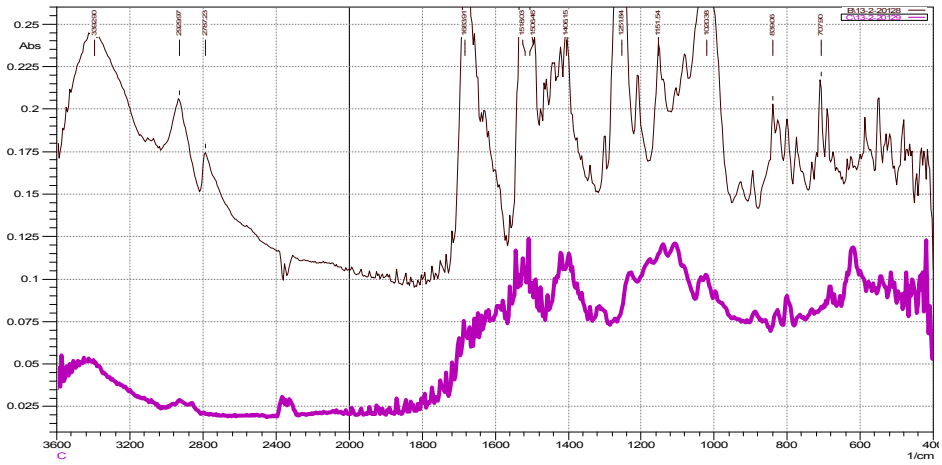

Figure 2: FT-IR spectra of activated *FSC* a) before, and b) after adsorption of CV dye.

3.2. SEM analysis

The surface of adsorbent was also characterized by scanning electron microscopy (SEM) before and after the adsorption experiments using the CV dye.

SEM images of the FSC (Figure 3(a)) showed bright dark color on the surface. After CV dye adsorption the surface of the FSC was turned to light color (Figure 3(b)). This may be due to the adsorption of CV dye on the surface of the FSC.

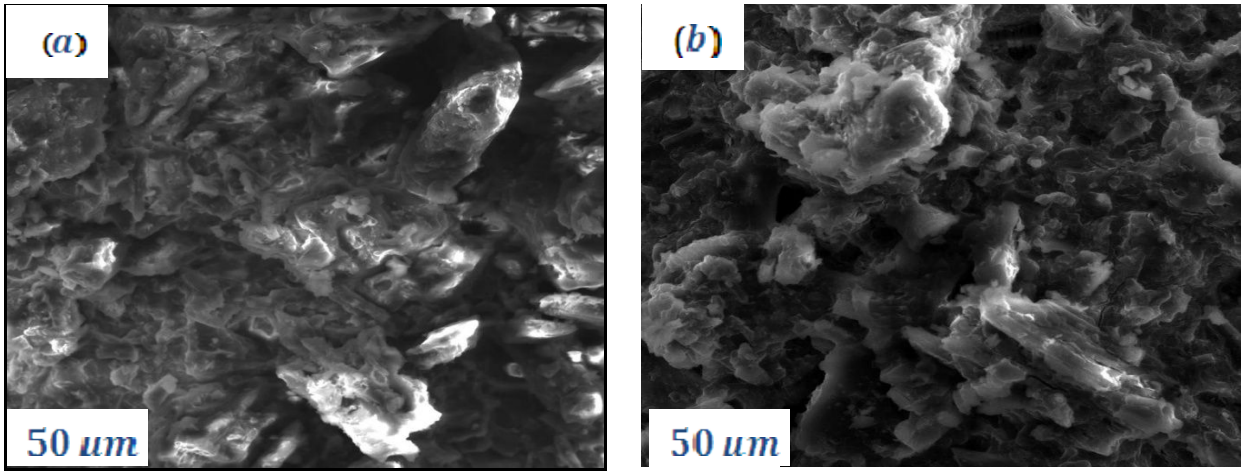

Figure 3. SEM image of activated *FSC* (a) before and (b) after adsorption of CV dye.

3.3 Effect of adsorbent dose

The study was carried out to examine the effect of *FSC* dose on the CV dye removal (adsorption) at 25 ^{o}C. Fig. 4 exhibits that the percentage removal of dye increased with an increase in the carton dose (0.005–0.1 g/L).

It is apparent that by increasing the adsorbent dose the amount of adsorbed dye increases but adsorption capacity, the amount adsorbed per unit mass, decreases. It is readily understood that the number of available adsorption sites increases by increasing the adsorbent dose and it, therefore, results in an increase of the amount of adsorbed dye. The decrease in adsorption capacity with an increase in the adsorbent dose is mainly because of adsorption sites remain unsaturated during the adsorption reaction whereas the number of sites available for adsorption site increases by increasing the adsorbent dose[38].

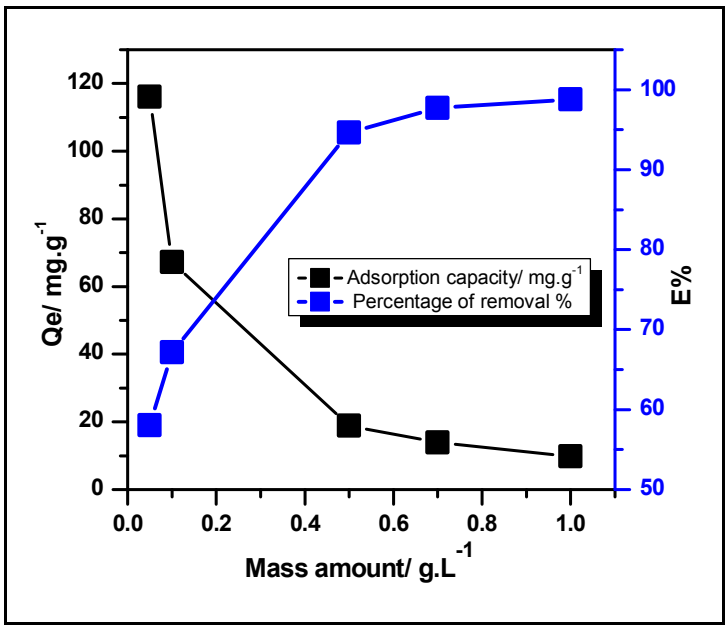

Fig.4: Effect of mass amount of adsorbent *FSC* on the percent removal and amount of adsorbed CV dye.

3.4 Effect of particle size

Particle size of an adsorbent played a very important role in the adsorption capacity of dye. The relationship of adsorption capacity to particle size depends on two criteria: (i) the chemical structure of the dye molecule (its ionic charge) and its chemistry (its ability to form hydrolyzed species) and (ii) the intrinsic characteristic of the adsorbent (its crystallinity, porosity and rigidity of the polymeric chains)[23]. Fig. 5 shows the effect of particle size on crystal violet adsorption. Results shows minimum particle size showed greater adsorption than larger size, increase in adsorption capacity with decreasing particle size suggests that the dye preferentially adsorbed on the outer surface and did not fully penetrate the particle due to steric hindrance of large dye molecules[39].

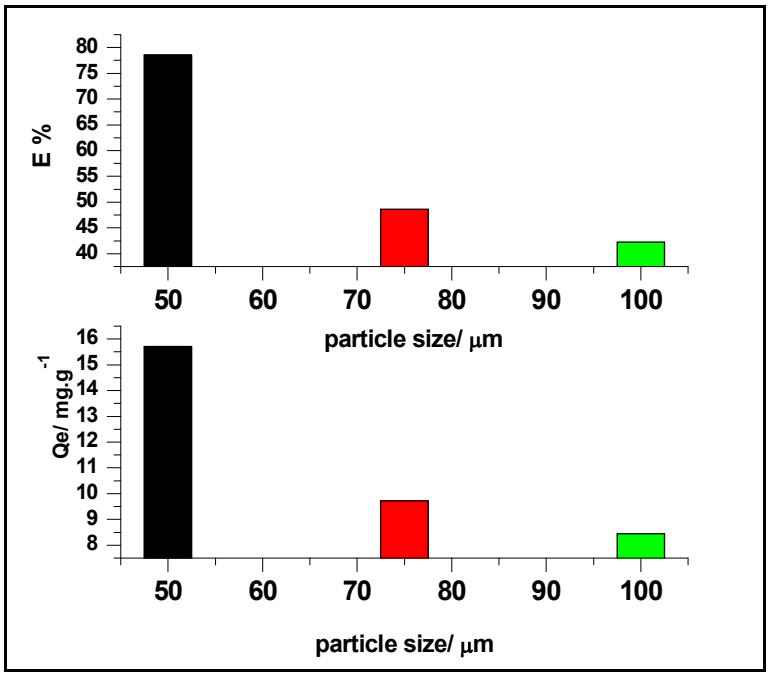

Fig.5: Effect of particle on the percent removal and amount of adsorbed CV dye onto *FSC* (crystal violet initial concentration = 10 mg/L, Temp. = 25°C, contact time 1 h, and mass of adsorbent 0.5 g/L).

3.5 Effect of solution pH on dye adsorption:

Numerous researchers have suggested the pH dependency of the basic dyes binding process on different materials[40]. The effect of pH on the adsorption of CV by the ***FSC*** is presented in Fig 6. The effect of pH on adsorption of dye was studied within pH range 2–10. Solution pH would affect both aqueous chemistry and surface binding-sites of the adsorbent. The equilibrium sorption capacity was minimum at pH 2 (6.5mg/g) and increased up to pH 10, reached maximum (17.34 mg/g) over the initial pH 2–10 The absence of sorption at low pH can be explained by the fact that at this acidic pH, H^+ may compete with dye ions for the adsorption sites of adsorbent, thereby inhibiting the adsorption of dye. At higher solution pH, the ***FSC*** may get negatively charged, which enhances the positively charged dye cations through electrostatic forces of attraction. Similar results of pH effect were also reported for the adsorption of CV onto jute carton [41] and dried activated sludge[42].

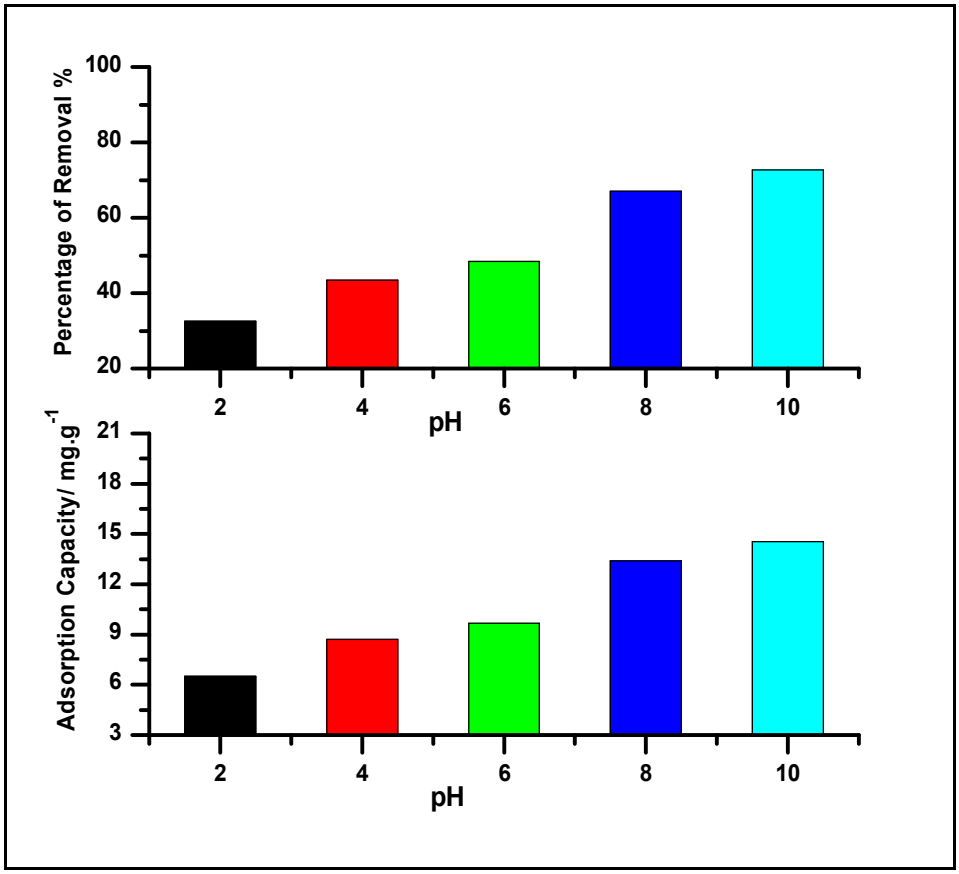

Fig.6: Effect of solution pH on the percent removal and amount of adsorbed CV dye onto *FSC* (crystal violet initial concentration = 10 mg/L, Temp. = 25°C, contact time 1 h, and mass of adsorbent 0.5 g/L).

3.6 Effect of initial CV concentration

The initial concentration provides an important driving force to overcome all mass transfer resistances of all molecules between the aqueous and solid phases. The initial concentrations of CV solutions were changed and time intervals were assessed until no adsorption of adsorbate on carton takes place.

Fig. 7 shows the effects of different initial CV concentrations on the adsorption capacity and removal efficiency of *FSC*. As shown, the adsorption capacity (Qe) increase with increasing initial CV concentration, while the percentage of removal decreasing with initial dye concentrations. The removal of dye by adsorption on *FSC* was found to be rapid low concentrations of dye and then to slow down with increasing in dye concentration. This was caused by attractive forces between the dye molecule and the adsorbent such as Van der Waals forces and electrostatic attractions; fast diffusion onto the external surface was followed by fast pore diffusion into the intraparticle matrix, which contains the chromophere groups such as alcoholic, carbonylic and phenolic occurring of the adsorption, to attain rapid equilibrium. In fact, the more concentrated the solution, the better the adsorption[43]. In other words, an increase in the surface loading led to a decrease in the adsorption rate.

Generally, when adsorption involves a surface reaction process, the initial adsorption is rapid. Then, a slower adsorption would follow was the available adsorption sites gradually decrease[26].

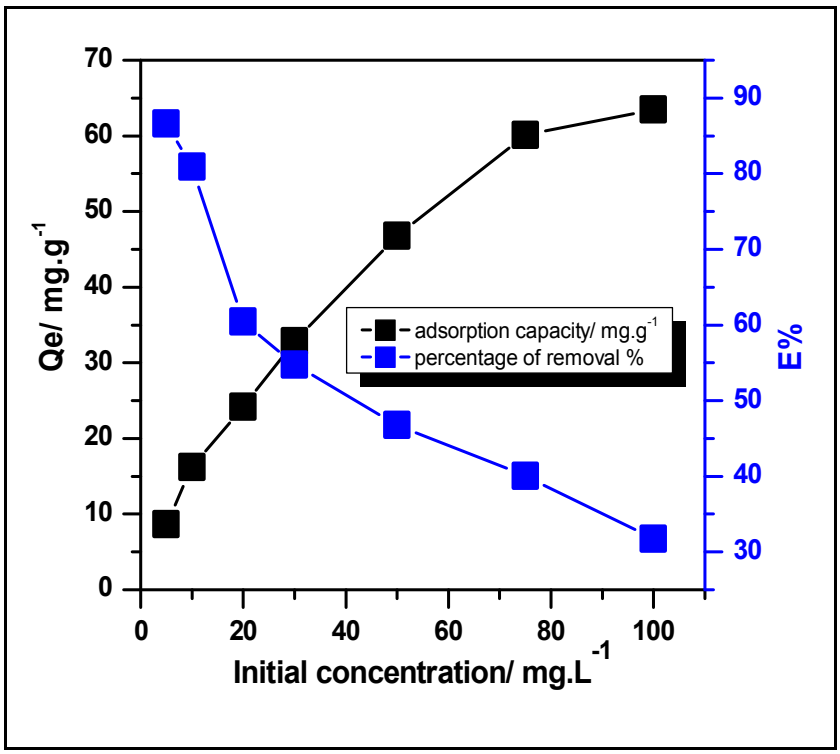

Fig.7: Effect of initial concentration on the percent removal and amount of adsorbed CV dye onto *FSC* (Exp. Condition: Temp. = 25°C, contact time 1 h, and pH of solution 6).

3.7. Models of Adsorption Isotherm

To investigate the parameters dependency of the adsorption capacity, three equilibrium models were analyzed, including Langmuir, Freundlich and Temkin. All the isotherms were simulated using an iterative procedure based on a non-linear least-squares algorithm. The Langmuir adsorption isotherm equation, expressed as follows requires for its applicability a mono-layered coverage on the surface of adsorbent[44]:

$$q_e = \frac{q_{\max} K_L C_e}{1 + K_L C_e} \qquad (3)$$

where q_e, K_L, q_{max} and C_e are uptake at equilibrium (mg g^{-1}), the Langmuir constant (L mg^{-1}), the monolayer adsorption capacity (mg g^{-1}) and the solution concentration at equilibrium (mg L^{-1}), respectively.

The Freundlich equation is applicable for multi component adsorption. The Freundlich isotherm is expressed by[45]:

$$q_e = K_F . C_e^{\frac{1}{n}} \qquad (4)$$

where K_F is the Freundlich constant ($mg^{1-1/n}\, L^{1/n}\, g^{-1}$) and n is the Freundlich exponent.

The non-linearized form of Temkin isotherm is represented by Eqn (5):

$$q_e = \frac{RT}{b} \log(K_T C_e) \qquad (5)$$

where b Temkin constant related to the heat of adsorption(kJ/mol), R : Gas constant (8.314 J/mol.K), T : Temperature (K), and K_T : Empirical Temkin constant related to the equilibrium binding constant related to the

maximum binding energy either (L/mg) or (L/mol). The adsorption data can be analyzed according to plot of the qe versus log Ce enables the determination of the isotherm constants K_T and b.

The Temkin isotherm takes into account the effects of the interaction of the adsorbate and the adsorbing species. By ignoring the extremely low and large concentration values, the model assumes that the heat of adsorption (a function of temperature) of all of the molecules in the layer would decrease linearly rather than logarithmically with coverage due to adsorbate-adsorbent interactions[46]. By comparing the three models, it seems that the model of Freundlich is the most adapted for the fitting of adsorption isotherms, then Langmuir model more adapted than Temkin model. Results are shown in (Fig. 8), the calculated parameters of three models are illustrated in Table 2.

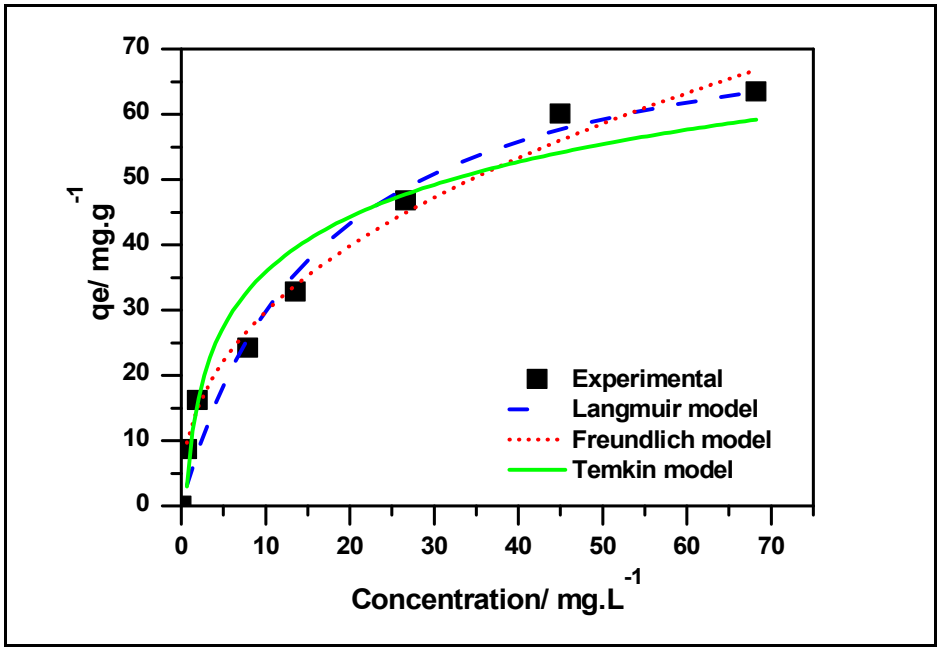

Fig. 8. Different adsorption isotherm models non linear fit for adsorption of CV dye on FSC (Experiment conditions: pH 6 and mass dosage 0.5 g/L, 25 °C).

Table 2: Langmuir, Freundlich, and Temkin model isotherms parameters for CV adsorbed on the surface of *FSC* at 25 °C

Langmuir Constants		Freundlich Constants		Temkin Constants	
Q_{max} (mg.g^{-1})	78.690	K_F (mg$^{1-1/n}$ L$^{1/n}$ g^{-1})	1.263	b	7.821
K_L (L mg^{-1})	0.0609	1/n	0.421	K_T	12.166
R^2	0.9500	R^2	0.9815	R^2	0.9072

3.8. Effect of solution temperature:

Fig. (8a and 8b) shows the effect of solution temperature on the adsorption of CV dye by using *FSC* , it is clear that when the solution temperature increased the adsorption capacity and dye removal will increased, this behavior could be attributed by the thermodynamic parameters expression.

The thermodynamic parameters, including the free energy changes (ΔG^0), standard enthalpy changes (ΔH^0) and the entropy changes (ΔS^0) associated with the adsorption process, can be used to deduce the adsorption mechanism. They can be calculated by the dependence of thermodynamic equilibrium constant (K_d) on temperatures[47]:

$$\Delta G^0 = -RTlnK_d \qquad (6)$$

$$K_d = \frac{-\Delta H^0}{RT} + \frac{\Delta S^0}{R} \qquad (7)$$

The thermodynamic equilibrium constant (K_d) for the adsorption of CV on *FSC* can be calculated using the equation[48]:

$$K_d = \frac{q_e}{C_e} \qquad (8)$$

The calculated values of K_d and the correlation coefficients are listed in Table 3.

The value of ΔH^0 and ΔS^0 can be calculated from the slope and intercept of the van't Hoff plot (Equation. (7)) of ln K_d against $1/T$, respectively, and the results are shown in (Fig. 8c) and listed in Table 3. The positive value of ΔH^0 indicates that the adsorption processes are endothermic. When attraction between adsorbates and an adsorbent took place, the change in standard enthalpy was caused by various forces, including van der Waals, hydrophobicity, hydrogen bonds, ligand exchange, dipole–dipole interactions and chemical bonds. According to Equation. (6), the values of ΔG^0 were calculated and listed in Table 3. The values of ΔG^0 of dye *FSC* adsorption systems are all negative, which indicates the spontaneous adsorption processes. Moreover, the increase in the absolute value of ΔG^0 with increasing temperature indicates that higher temperatures facilitated the adsorption.

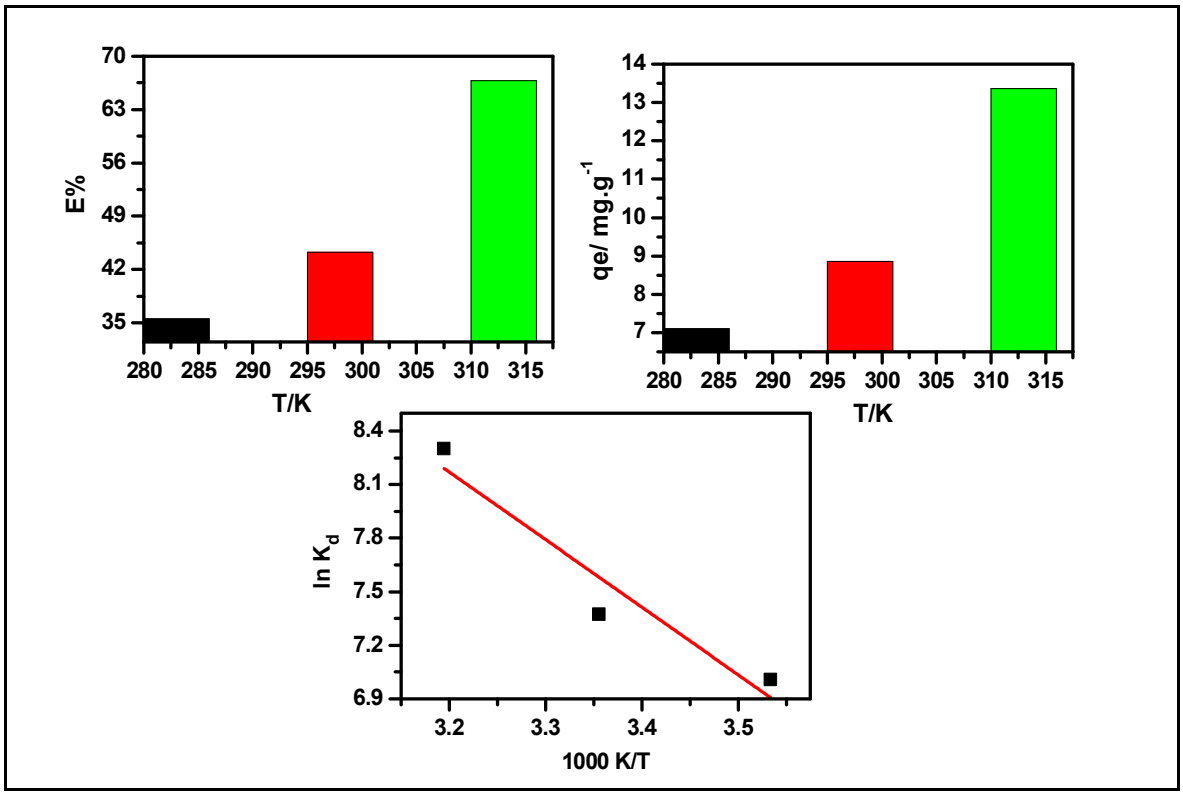

Fig. 9: Effect of solution temperature on adsorption of CV by *FSC* a) percentage of removal, b) adsorption capacity and c) linear plots for determination thermodynamic parameters.

Table 3: Thermodynamics parameters for adsorption of CV dye by *FSC* surface.

Temp/ K	K_d	ΔG^0/ kJ.mol^{-1}	ΔH^0/ kJ.mol^{-1}	ΔS^0/ J.K.$^{-1}$mol^{-1}
283	1103.2	-16.48	31.5284	168.83
298	1590.8	-18.26		
313	4027.4	-21.60		

4. Conclusion

The adsorption equilibrium of the CV dye on the *FSC* was studied in a batch mode operation for the parameters initial dye concentration, pH of solution, particle size, temperature, and adsorbent dosage. The results showed that adsorption of the dye increased with increase in initial dye concentrations, temperature and pH while it decreased with increase in adsorbent mass and particle size. The adsorption equilibrium isotherms were analyzed by Langmuir, Freundlich, and Temkin isotherm equations. All results obeying isotherm models were choosing in this study but more favourable for Freundlich which provided the best correlations for the CV dye onto *FSC*. As a result of the thermodynamic evaluation of CV adsorption, the obtained negative ΔG values revealed that the adsorption of CV onto *FSC* was thermodynamically feasible and spontaneous, the positive values of ΔH suggested the endothermic nature of adsorption, and the positive values of ΔS indicated the increasing randomness at the solid/solution interface during the adsorption process.

References:

1. Al-Degs Y., Khraisheh M. A. M., Allen S. J., and Ahmad M. N., 2000. Effect of carbon surface chemistry on the removal of reactive dyes from textile effluent, Water Research, 34: 927-935.
2. Prola L. T., Acayanka E., Lima E. C., Umpierres C. S., Vaghetti J. P., Santos W. O., Laminsi S., and Djifon P. T., 2013. Comparison of Jatropha curcas shells in natural form and treated by non-thermal plasma as biosorbents for removal of Reactive Red 120 textile dye from aqueous solution, Ind. Crop. Prod., 46: 328-340.
3. Nigam P., Armour G., Banat I. M., Singh D., and Marchant R., 2000. Physical removal of textile dyes from effluents and solid-state fermentation of dye-adsorbed agricultural residues, Bioresource Technology, 72: 219-226.
4. Cardoso N. F., Lima E. C., Pinto I. S., Amavisca C. V., Royer B., Pinto R. B., Alencar W. S., and Pereira S. F. P.,, 2011. Application of cupuassu shell as biosorbent for the removal of textile dyes from aqueous solution, Journal of Environmental Management, 92: 1237-1247.
5. Robinson T., McMullan G., Marchant R., and Nigam P., 2001. Remediation of dyes in textile effluent: a critical review on current treatment technologies with a proposed alternative, Bioresource Technology, 77: 247-255.
6. Moussavi, G.; Mahmoudi, M., 2009. Degradation and biodegradability improvement of the reactive red 198 azo dye using catalytic ozonation with MgO nanocrystals, Chemical Engineering Journal, 152: 1-7.
7. Asgher M., and Bhatti N. H., 2012. Removal of reactive blue 19 and reactive blue 49 textile dyes by citrus waste biomass from aqueous solution: Equilibrium and kinetic study, Can. J. Chem. Eng., 90: 412-419.
8. Alkaim A. F., Aljeboree A. M., Alrazaq N. A., Baqir S. J., Hussein F. H., and Lilo A. J., 2014. Effect of pH on Adsorption and Photocatalytic Degradation Efficiency of Different Catalysts on Removal of Methylene Blue, Asian Journal of Chemistry, 26: 8445-8448.
9. Algubili A. M., Alrobayi E. M., and Alkaim A. F., 2015. Photocatalytic degradation of remozal briliant blue dye by ZnO/UV process, Int. J. Chem. Sci., 13: 911-921.
10. Al-Gubury H. Y., and Al-Murshidy G. S., 2015. Photocatalytic Decolorization of Brilliant Cresyl Blue using Zinc Oxide International Journal of PharmTech Research, 8: 289-297.
11. Mohamed F. F., Allah P. M., Mehdi A. P., and Baseem M. , 2011. Photoremoval of Malachite Green (MG) using advanced oxidation process, Res.J.Chem.Environ., 15: 65-70.
12. Mashkour M. S., Al-Kaim A. F., Ahmed L. M., and Hussein F. H., 2011. Zinc oxide assisted photocatalytic decolorization of reactive red 2 dye, Int. J. Chem. Sc., 9: 969-979.
13. Alkaim A. F., and Hussein F. H., 2012. Photocatalytic degradation of EDTA by using TiO_2 suspension, Int J Chem Sci, 10: 586-598.

14. Enas M. Alrobayi, Abrar M. Algubili, Aseel M. Aljeboree, Ayad F. Alkaim, and Falah H. Hussein, DOI: 10.1080/02726351.2015.1120836. Investigation of Photocatalytic Removal and Photonic Efficiency of Maxilon Blue Dye GRL in the Presence of TiO2 Nanoparticles, Particulate Science and Technology.
15. Karam F. F., Kadhim M. I., and Alkaim A. F. , 2015. Optimal conditions for synthesis of 1, 4-naphthaquinone by photocatalytic oxidation of naphthalene in closed system reactor, Int. J. Chem. Sci., 13: 650-660.
16. Kandiel T. A., Robben L., Alkaim A., and Bahnemann D., 2013. Brookite versus anatase TiO_2 photocatalysts: phase transformations and photocatalytic activities, Photochem. Photobiol. Sci., 12: 602-609.
17. Alkaim, A. F.; Kandiel, T. A.; Hussein, F. H.; Dillert, R.; Bahnemann, D. W., 2013. Solvent-free hydrothermal synthesis of anatase TiO2 nanoparticles with enhanced photocatalytic hydrogen production activity, Applied Catalysis A: General 466: 32-37.
18. Alkaim, A. F.; Kandiel, T. A.; Hussein, F. H.; Dillert, R.; Bahnemann, D. W., 2013. Enhancing the photocatalytic activity of TiO2 by pH control: a case study for the degradation of EDTA, Catal. Sci. Technol., 3: 3216–3222.
19. Alkaim, A. F., Dillert, R., and Bahnemann, D. W., 2015. Effect of polar and movable (OH or NH2 groups) on the photocatalytic H2 production of alkyl-alkanolamine: a comparative study, Environ. Technol., 36: 2190–2197.
20. Alkaim A. F., Sadik Z., Mahdi D. K., Alshrefi S. M., Al-Sammarraie A. M., Alamgir F. M., Singh P. M., and Aljeboree A. M., 2015. Preparation, structure and adsorption properties of synthesized multiwall carbon nanotubes for highly effective removal of maxilon blue dye, Korean J. Chem. Eng., 32: 2456-2462.
21. Hadi Z. A., Aljeboree A. M. and Alkaim A. F., 2014. Adsorption of a cationic dye from aqueous solutions by using waste glass materials: isotherm and thermodynamic studies, Int. J. Chem. Sci., 12: 1273-1288.
22. Aljeboree A. M., Radi N., Ahmed Z., and Alkaim A. F., 2014. The use of sawdust as by product adsorbent of organic pollutant from wastewater: adsorption of maxilon blue dye, Int. J. Chem. Sci., 12: 1239-1252.
23. Aljeboree A. M., Alshirifi A. N., and Alkaim A. F., 2014. Kinetics and equilibrium study for the adsorption of textile dyes on coconut shell activated carbon, Arabian J. Chem., 10.1016/j.arabjc.2014.01.020.
24. Alkaim A. F., and Alqaragully M. B. , 2013. Adsorption of basic yellow dye from aqueous solutions by Activated carbon derived from waste apricot stones (ASAC): Equilibrium, and thermodynamic aspects, Int. J. Chem. Sc., 11: 797-814.
25. Aljeboree A. M., 2015. Adsorption of methylene blue dye by using modified Fe/Attapulgite clay., Research Journal of Pharmaceutical, Biological and Chemical Sciences 6: 778-788.
26. Aljeboree A. M., Alkaim A. F., and Al-Dujaili A. H., 2015. Adsorption isotherm, kinetic modeling and thermodynamics of crystal violet dye on coconut husk-based activated carbon, Desalin. Water Treat., 53: 3656-3667.
27. Aljebori, A. M.; Alshirifi, A. N., 2012. Effect of Different Parameters on the Adsorption of Textile Dye Maxilon Blue GRL from Aqueous Solution by Using White Marble, Asian journal of chemistry, 24: 5813-5816
28. El-Gohary F., and Tawfik A., 2009. Decolorization and COD reduction of disperse and reactive dyes wastewater using chemical-coagulation followed by sequential batch reactor (SBR) process, Desalination, 249: 1159-1164.
29. Dâas A., and Hamdaoui O., 2010. Extraction of anionic dye from aqueous solutions by emulsion liquid membrane, J. Hazard. Mater., 178: 973-981.
30. Wang L., 2009. Aqueous organic dye discoloration induced by contact glow discharge electrolysis, J. Hazard. Mater., 171: 577-581.
31. El-Naas M. H., Al-Muhtaseb S. A., and Makhlouf S., 2009. Biodegradation of phenol by Pseudomonas putida immobilized in polyvinyl alcohol (PVA) gel, J. Hazard. Mater., 164: 720-725.
32. Chakraborty S., Purkait M. K., Das S., Gupta S., De S., and Basu J. K., 2003. Nanofiltration of textile plant effluent for color removal and reduction in COD, Sep. Purif. Technol., 31: 141-151.

33. Shi H., Li W., Zhong L. and Xu C. , 2014. Methylene Blue Adsorption from Aqueous Solution by Magnetic Cellulose/Graphene Oxide Composite: Equilibrium, Kinetics, and Thermodynamics, Ind. Eng. Chem. Res., 53: 1108-1118.
34. Lakshmi U. R., Srivastava V. C., Mall I. D., and Lataye D. H., 2009. Rice husk ash as an effective adsorbent: Evaluation of adsorptive characteristics for Indigo Carmine dye, J. Environ. Manage., 90: 710-720.
35. Djilani C., Zaghdoudi R., Djazi F., Bouchekima B., Lallam A., Modarressi A., and Rogalski M., 2015. Adsorption of dyes on activated carbon prepared from apricot stones and commercial activated carbon, Journal of the Taiwan Institute of Chemical Engineers, 53: 112-121.
36. Hameed B. H., Mahmoud D. K., and Ahmad A. L., 2008. Equilibrium modeling and kinetic studies on the adsorption of basic dye by a low-cost adsorbent: Coconut (Cocos nucifera) bunch waste, J. Hazard. Mater., 158: 65-72.
37. Abd El Hakim, T. K.; Ebtssam, A. S.; Ayman, A. A.; Amir, E. A., 2012. Study on adsorption behavior and separation efficiency of naturally occurring clay for some elements by batch experiments, European Journal of Chemistry, 1: 99-105.
38. Malik, R., Ramteke, D.S., Wate, S.R., , 2007. Adsorption of malachite green on groundnut shell waste based powdered activated carbon. . , Waste Manage, 27: 1129-1138.
39. Gouamid M., Ouahrani M. R., and Bensaci M. B., 2013. Adsorption Equilibrium, Kinetics and Thermodynamics of Methylene Blue from Aqueous Solutions using Date Palm Leaves, Energy Procedia, 36: 898-907.
40. Weng C., and Pan Y., 2007. Adsorption of a cationic dye (methylene blue) onto spent activated clay, Journal of Hazardous Materials, 144: 355-362.
41. Liqiang Jin a, Qiucun Sun b, Qinghua Xu b, Yongjian Xu 2015. Adsorptive removal of anionic dyes from aqueous solutions using microgel based on nanocellulose and polyvinylamine Bioresource Technology: 348-355.
42. Senthilkumaar S., Varadarajan P. R., Porkodi K., and Subbhuraam C. V., 2005. Adsorption of methylene blue onto jute fiber carbon: kinetics and equilibrium studies, J. Colloid Interface Sci., 2854: 78–82.
43. Bulut Y., and Aydın H., 2006. A kinetics and thermodynamics study of methylene blue adsorption on wheat shells, Desalination, 194: 259-267.
44. Langmuir I., 1918. Adsorption of gases on plain surfaces of glass mica platinum, J. Am. Chem. Soc., 40: 1361–1403.
45. Freundlich H. M., 1906. Over the adsorption in solution, J. Phys. Chem., 57: 385-470.
46. Aharoni C., and Ungarish M., 1977. Kinetics of activated chemisorption. Part 2. Theoretical models, J. Chem. Soc., Faraday Trans., 73: 456-464.
47. Li, Q.; Yue, Q.; Su, Y.; Gao, B.; , S., H., 2010. Equilibrium, thermodynamics and process design to minimize adsorbent amount for the adsorption of acid dyes onto cationic polymer-loaded bentonite, Chem. Eng. J., 158: 489-497.
48. Gupta, V. K.; Singh, P.; , R., N., 2004. Adsorption behavior of Hg(II), Pb(II), and Cd(II) from aqueous solution on Duolite C-433: a synthetic resin, J. Colloid Interface Sci., 275: 398-402.

*****